Interactions between bed forms: Topography, turbulence, and transport

Douglas Jerolmack and David Mohrig

Department of Earth, Atmospheric and Planetary Sciences, Massachusetts Institute of Technology, Cambridge, Massachusetts, USA

Received 26 January 2004; revised 14 March 2005; accepted 31 March 2005; published 16 June 2005.

[1] Results are presented examining the interaction between two sandy bed forms under low–sediment transport conditions in a small laboratory flume. The initial artificially made bed forms were out of equilibrium with the flow field. Temporal evolution of bed forms was monitored using time-lapse photography in order to characterize bed form adjustment to the imposed flow. Velocity measurements were collected using an acoustic Doppler velocimeter to characterize both mean flow and turbulence associated with different bed form geometries. Sandy bed forms all had identical initial geometries; however, the initial distance between bed form crests was varied between experiments. Overall deformation of the bed varied as a function of initial bed form spacing; however, bed forms evolved unpredictably as periods of relatively slow change were punctuated by periods of rapidly changing geometry. Subtle changes in bed form trough geometry were found to have a strong influence on turbulence and therefore sediment transport. Comparison with field studies suggests that the mechanisms described herein are active in natural systems.

Citation: Jerolmack, D., and D. Mohrig (2005), Interactions between bed forms: Topography, turbulence, and transport, *J. Geophys. Res.*, *110*, F02014, doi:10.1029/2004JF000126.

1. Introduction

[2] As techniques improve for collecting topographic data at higher temporal and spatial resolutions, evidence is mounting for the persistence of locally variable topography and sediment fluxes under steady or slowly varying hydraulic conditions. For example, a recent laboratory study of dunes by *Leclair* [2002] documented continuously adjusting geometries for individual bed forms and continuously adjusting rates of migration even after the system had been allowed to interact with a constant hydraulic forcing for as long as 24 hours. The exhaustive field study on bed forms of the River Rhine by *Carling et al.* [2000a, 2000b] produced a comparable result. Measured bed form topography there could not be linked to river stage in a simple way. Laboratory data by *Ditchfield and Best* [1992] have shown that migration rate for individual bed forms can depart significantly from values predicted using the channel-averaged measurement of sediment flux. These results and others (e.g., river studies by *van den Berg* [1987], *Mohrig* [1994], *Harbor* [1998], and *Prent and Hickin* [2001]) lead us to conclude that persistent variability in geometry and migration rates are not the exception, but are in fact the hallmark of natural bed forms developing under and interacting with unidirectional shear flows.

[3] Bed forms are created and modified by variations in the sediment flux. Their presence induces flow accelerations, which, in turn, modulate the sediment flux [*Nelson et al.*, 1993]. Fortunately, careful work on pieces of these interactions provides a framework for understanding the feedbacks. Particularly useful are the detailed measurements defining spatial heterogeneity in the flow field over static two-dimensional [*Engel*, 1981; *Wiberg and Nelson*, 1992; *Nelson et al.*, 1993; *McLean et al.*, 1994] and three-dimensional [*Maddux et al.*, 2003a, 2003b] bed forms in the laboratory, and over quasi-static dunes in large rivers [*Kostaschuk*, 2000]. Laboratory measurements have mapped out the zones of turbulence production and dissipation over bed forms, and have defined the associated variability in turbulence intensities. These measurements provide critical information as to why natural topography continuously evolves even under steady flow conditions: local values of turbulence intensity are sensitive to local accelerations in the flow and these accelerations are sensitive to local slopes of the bed form surface. In addition, local rates of bed load transport have been shown to be sensitive to high-velocity bursts [*Schmeeckle and Nelson*, 2003; *Best et al.*, 1997]. Taken together, these conditions are the ingredients of a recipe for topographic evolutions that are extremely sensitive to boundary conditions. The geometries of an individual bed form will always be evolving in response to its previous form, as well as in response to the structure of the surrounding bed.

[4] Several simple numerical models of subaqueous [e.g., *Tufillaro*, 1993; *Niño et al.*, 2002] and subaerial [e.g., *Prigozhin*, 1999; *Csahók et al.*, 2000] bed forms have succeeded in capturing aspects of bed form development

0148-0227/05/2004JF000126$09.00

Table 1. Grain Size of the Medium and Coarse Sand, Where d_{10}, d_{50}, and d_{90} Refer to the 10, 50, and 90 Cumulative Percentile

Class	Medium Sand	Coarse Sand
d_{10}	270 μm	475 μm
d_{50}	350 μm	770 μm
d_{90}	510 μm	945 μm

from an initially flat surface, such as amplitude growth and merging of bed forms; however, in these formulations bed form evolution is governed by irreversible merger of individual topographic elements [see also *Werner and Gillespie*, 1993] such that bed form wavelength can only increase it time. *Werner and Kocurek* [1999] suggested the spacing of bed forms is controlled by the dynamics of defects (crest line terminations); however, the creation and annihilation of defects is a natural consequence of spatial variation in sediment flux, which was not considered in their model. Although recent numerical [*Hersen et al.*, 2004] and experimental [*Endo et al.*, 2004] work suggests that individual barchan dunes are dynamically unstable, we are far from understanding the source of bed form instability and its contribution to the maintenance of trains of bed forms.

[5] The goal of the experiments reported here was to examine how bed forms interact when forced to adjust to an imposed flow field, and to describe the interaction among spatially varying flow and sediment transport and changes in bed form geometry.

[6] The geometric variability of bed forms themselves confounds the proper choice of length and timescales for use in generating accurate descriptions of bed evolution. To minimize these complications, we have run a set of experiments using very simple initial geometries. Bed forms were artificially created that were out of equilibrium with the flow field. The importance of small-scale interactions between bed forms was brought to the fore in these ''extreme conditions.'' The bed geometries have allowed us to unambiguously identify the influences of one bed form on another. Results presented here summarize the control of initial spacing between two sandy bed forms on subsequent bed evolution in a two-dimensional channel. To do this the bed form spacing was systematically varied while all other parameters were held constant. Adjustments of individual bed forms directly affected many aspects of the bed configuration, highlighting the need to collect both high-resolution spatial and temporal data when characterizing river bottom topography. Periods of rapid local deformation for individual bed forms are connected to subtle changes in local topography, and to the changes in turbulence intensities and sediment transport that they produced. Throughout this paper, ''bed configuration'' and ''bed profile'' will be used interchangeably to refer to the entire channel bottom topography, while ''bed form'' always refers to an individual topographic element, as defined in the Methods section below.

2. Methods

2.1. Experimental Setup

[7] The initial size and shape for all bed forms was held constant in our experiments. The height and length of each was 0.070 m and 0.395 m, respectively. Each bed form had no topographic variation in the cross-stream direction. The stoss side of each form was inclined at 13° from the horizontal, while inclination of the lee side was 35°. These bed forms were constructed out of two very different materials; aluminum plate and sand. Bed forms made from bent aluminum plate produced a fixed bed, necessary for sampling the velocity structure of the flow field. The aluminum forms also served as the moulds for generating the sandy bed forms. In these cases the channel was first filled with water and then water-saturated sand was pressed into forms of the equivalent shape and size using the moulds. These experiments were carried out with bed forms constructed from two different sands having median particle diameters of 350 μm and 770 μm, respectively (Table 1).

[8] Experiments were conducted in the middle third of a straight flume, 10 m long, 0.16 m wide and 0.25 m deep, with zero slope. The flume recirculated both water and sediment and a valve on the flume return line controlled discharges through the test channel. The narrow width of the flume may have influenced bed evolution, but no attempt has been made to quantify this effect. Four different configurations of the bed were studied in the test section (Figure 1). In the first case (Figure 1a) a single bed form was placed in the upstream position of the test reach. Results from this single-form case served as a baseline for comparison to the other configurations. A single bed form composed of medium and then coarse sand was used to set the water discharges applied to all of the other runs. Specifically, water discharges were adjusted until transport conditions were slightly above thresholds of initial particle motion for the two sands. The vertically averaged flow velocities associated with this transport stage are listed in Table 2. Under these conditions there was almost no translation and/or deformation of the single sandy bed form. Experimental runs having the same discharge, but with two bed forms in the channel, experienced different kinematic behaviors that are reported below.

[9] Three different bed form spacings were used (Figure 1 and Table 2). These were selected on the basis of velocity measurements collected over a single rigid form in the channel. These measurements characterized the structure of the flow field downstream of an obstruction (i.e., zones 1, 2, and 3 of Figure 1). In the first case two bed forms were positioned end to end, producing a configuration where part of the downstream form (bed form 2) was situated within the recirculation eddy that developed because of flow separation at the crest of bed form 1 (Figure 1b). In the second case the bed forms were sufficiently separated such that all of bed form 2 resided downstream from the point of flow reattachment (Figure 1c). For the final configuration the two forms were placed such that bed form 2 lay outside of the detectable range of disturbance of the flow field produced by a single upstream bed form (Figure 1d), as determined by measured mean and turbulent fluid velocity statistics. Our goal was to place the downstream bed form in three very different flow regimes using the three chosen spacings.

2.2. Measurement of Sandy Bed Forms

[10] The kinematic histories for the experimental bed forms were recorded using a digital camera taking pictures through a clear Plexiglas sidewall. These photographs were

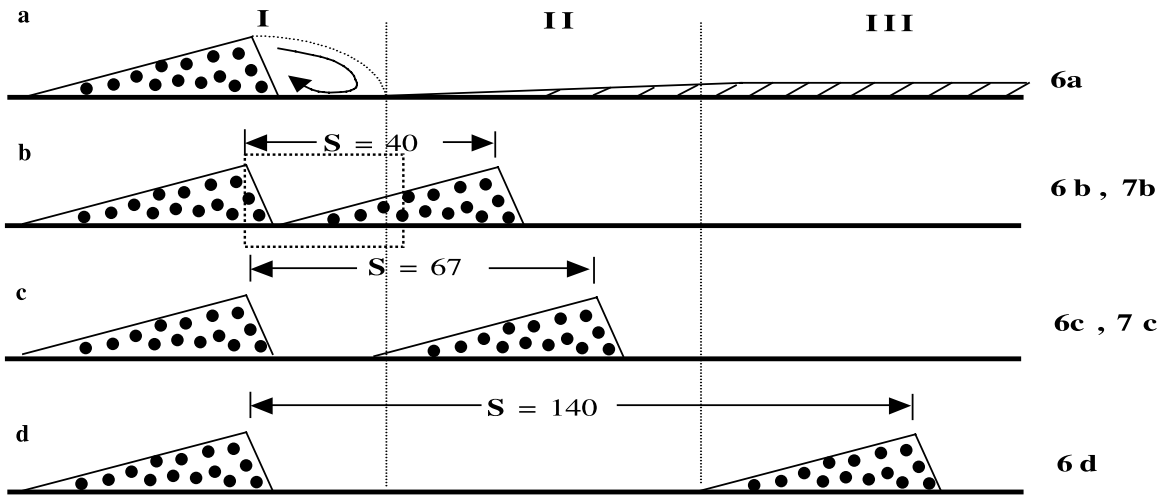

Figure 1. Bed configurations used in reported experiments. Labels at right of each plot indicate names of experimental runs with the given bed configuration; see also Table 2. (a) Single bed form. The flow field downstream from this single form is divided into three zones, as described in the text. (b) Back-to-back bed forms with crests separated by a spacing, s, equal to the bed form length. The dashed box demarcates the area where flow measurements were made (see Figure 10). (c) Two identical forms separated by a spacing of 0.67 m. (d), Two identical forms separated by a spacing of 1.40 m. Direction of flow is from left to right in Figures 1–11.

taken every 120 s for approximately 3 hours. Selected photographs were digitized using ImageJ, a public domain image processing and analysis program developed at the National Institutes of Health. Resulting digital images were then used to quantify both the translation and deformation of individual bed forms by measuring changes in height, H, length, L, cross-sectional area, A, and downstream position. The migration rate or celerity, c, of individual bed forms was calculated by measuring streamwise changes in the positions of bed form crests over short time intervals. Definitions for all of these properties are shown in Figure 2. Measurement precision was limited by the resolution of our photographs. Changes in bed elevation of $<5 \times 10^{-3}$ m could not be resolved. In addition, our method of data collection did not capture cross-stream variability in topography and migration rate. Such variability occurred in cases with medium-sand bed forms (Tables 1 and 2), but was nearly absent in the coarse-sand runs. Visual inspection of all bed forms led us to conclude that behaviors measured in cross section near the sidewall were representative of the overall kinematics despite some cross-stream variability associated with bed forms made of medium sand.

[11] The evolving topography in our experiments included the emergence and destruction of individual bed forms. Acknowledging that any definition of first appearance or disappearance of a discrete bed form is somewhat arbitrary, we decided on the following criteria: (1) The obtuse angle, θ, between the lee face of a new form and the adjacent downstream surface must be less than 150°; and (2) the height of a new form must be greater than one third the height of the bed form from which it developed (Figure 2). This definition separated bed forms from swales and hummocks, and separated smaller-scale superimposed topography from primary bed forms themselves. The smaller topographic elements, including ripples on the stoss sides of bed forms, were not considered separate entities (Figure 2) and were treated as simply contributing to the massiveness of the bed forms on which they resided. With this definition we mapped temporal change in bed form size, shape and number. In each trial run, values of H, L, H/L, A, and c were collected for all bed forms as a function of time. Average values for these parameters were then calculated in two different ways. A system average was calculated at each time step using all of the data from the run, and local averages were determined using only those measurements from bed forms sharing a common original parent (bed form 1 or bed form 2, Figure 1). These local measurements allowed us to evaluate how bed form kinematics varied as a function of position in the system. Statistics describing the deformation of individual bed forms as well as the overall evolution of the bed configuration were compiled for each trial, allowing us to assess the relative importance of initial bed form spacing, s, on developing local topography.

[12] At the beginning of each trial the only sand within the channel was that making up the bed forms. The channel

Table 2. Initial Conditions for All Experimental Runs[a]

Run	d_{50}, μm	S, m	$\bar{u}$, m/s	h, m	Q_f, m^2/s	Fr	Re
6a	350	···	0.27	0.191	5.2×10^{-2}	0.20	1.5×10^4
6b1	350	0.40	0.27	0.191	5.2×10^{-2}	0.20	1.5×10^4
6b2	350	0.40	0.27	0.192	5.2×10^{-2}	0.20	1.5×10^4
6b3	350	0.40	0.27	0.192	5.2×10^{-2}	0.20	1.5×10^4
6c1	350	0.67	0.27	0.191	5.2×10^{-2}	0.20	1.5×10^4
6c2	350	0.67	0.28	0.191	5.3×10^{-2}	0.21	1.6×10^4
6c3	350	0.67	0.27	0.191	5.2×10^{-2}	0.20	1.5×10^4
6d	350	1.40	0.27	0.189	5.1×10^{-2}	0.20	1.5×10^4
7b	770	0.40	0.32	0.192	6.1×10^{-2}	0.22	1.7×10^4
7c	770	0.67	0.32	0.192	6.1×10^{-2}	0.22	1.7×10^4

[a]Flow depth is h, width-averaged fluid discharge is Q_f, and calculated Froude and Reynolds numbers are Fr and Re, respectively. All other parameters are defined in text.

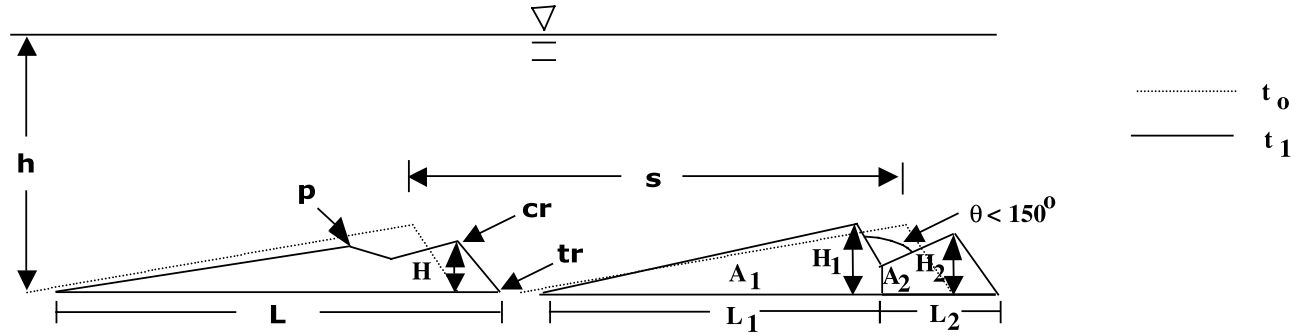

Figure 2. Definition sketch for experimental measurements. The bed form configuration is shown both at the beginning of an experiment (t_0) and at some later time (t_1). Bed form features include crest, *cr*; trough, *tr*; and peak (a local topographic high that is not a bed form crest), *p*. A_1 and A_2 are the cross-sectional areas associated with two separate bed forms originating from a single parent form. All other parameters are defined in the text.

floor both upstream and downstream from the bed forms consisted of smooth Plexiglas. This immobile surface was also exposed between bed forms in those cases where the spacing, *s*, was greater than the bed form length, *L* (Figures 1c and 1d). We limited the amount of sand in the system in an attempt to isolate and highlight the interactions between two original bed forms. In cases with only a single bed form made from medium sand (case 6a) and two forms separated by 1.40 m (case 6d), only one run was used to characterize bed evolution. However, in order to assess reproducibility and sensitivity to boundary conditions, three runs were conducted for each of the highly variable scenarios of s = 0.40 m (case 6b) and s = 0.67 m (case 6c). Only these two configurations of the bed were rerun using the coarse sand: cases 7b and 7c, respectively (Figure 1 and Tables 1 and 2). Successive profiles of the bed for selected runs using medium sand are shown in Figure 3.

[13] Changes in bed topography during the first 1920 s of every trial were used to estimate local values for the

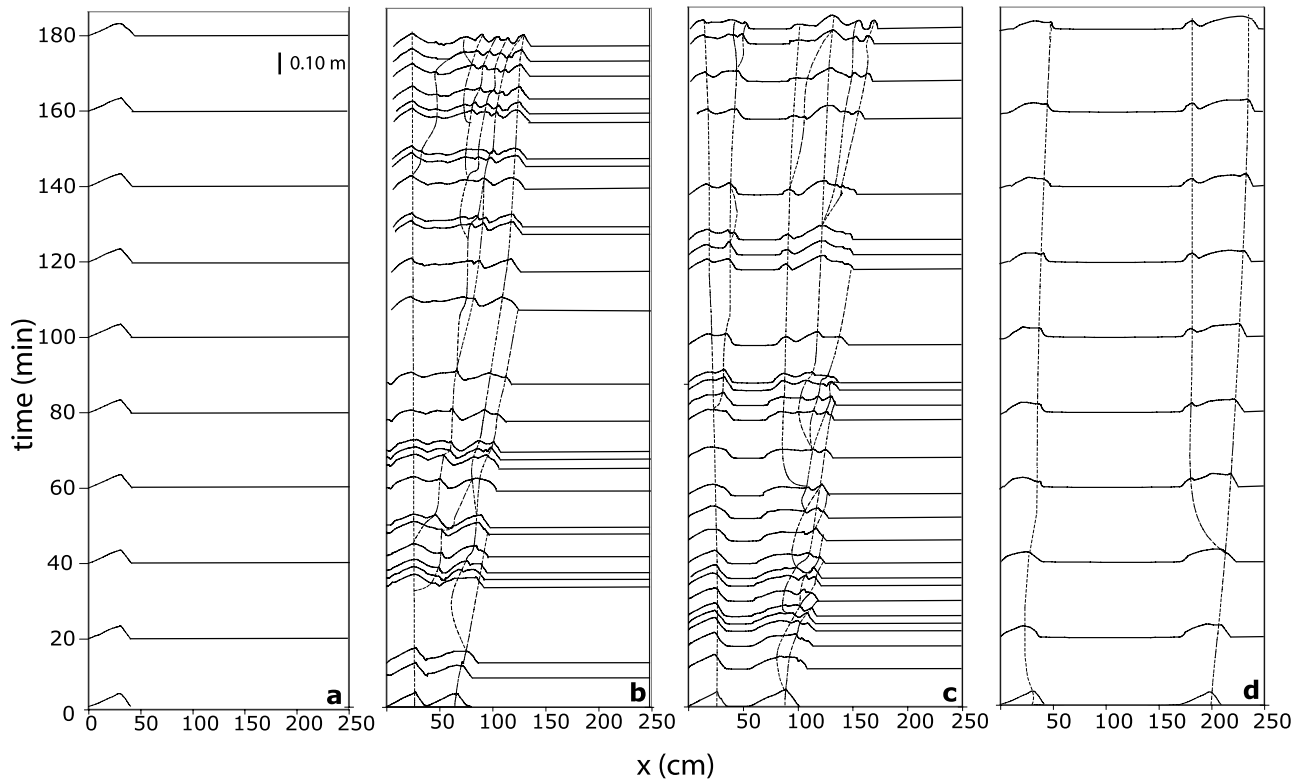

Figure 3. Profiles of bed forms as a function of time for (a) run 6a, (b) run 6b3, (c) run 6c3, and (d) run 6d. Each time series is built using the smallest number of profiles necessary to capture significant change in both the positions of crests and bed form number. Dashed lines connect the same crest on successive profiles. The beginning and ending of dashed lines mark the splitting and merging of individual bed forms, respectively. Vertical scale bar is shown in Figure 3a.

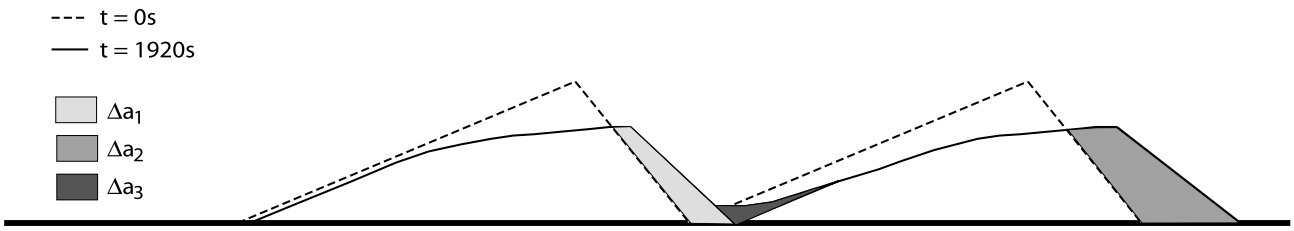

Figure 4. Changes in bed topography through time used to calculate local values for streamwise sediment discharge, q_s (equation (1)). The newly generated cross-sectional areas used to determine q_s at the crests of bed form 1 and bed form 2 are Δa_1 and Δa_2, respectively. The cross-sectional area used to determine the upstream transport filling in the trough of bed form 1 is Δa_3.

streamwise sediment discharge, q_s. These values were calculated using the following equation

$$q_s = \Delta a(1 - k)/\Delta t \tag{1}$$

where Δa is newly created bed form area (Figure 4), k is porosity, and Δt is the time interval over which the new area was created. Equation (1) was used to estimate the streamwise sediment flux at three locations in the system: (1) the stoss side of bed form 1; (2) the stoss side of bed form 2; and, when appropriate, (3) the trough separating bed form 1 from bed form 2 (Figure 4). This calculation assumes that no grains bypassed the bed forms completely (i.e., suspension was negligible) in the study region. Values of q_s for trough filling are negative, representing the upstream transport of sediment associated with the recirculation eddy that developed behind bed form 1 (Figure 1). Trough-filling values of q_s were only measured for cases where an immediate source of sediment was available for trough filling, i.e., the stoss side of bed form 2 (cases 6b and 7b, Table 2). Sediment flux calculations were not performed using data from the last 2.5 hours of each run because the splitting and merging of bed forms made it difficult to integrate Δa over intervals of time sufficient in duration to produce representative measures of sediment discharge.

2.3. Measurement of Flow Field

[14] All velocity measurements were collected using a Sontek acoustic Doppler velocimeter (micro-Lab ADV) running at a sampling frequency of 10 Hz. The sampling volume for this device was small, 10^{-6} m^3, so the flow fields for specific runs were characterized by measuring successive vertical profiles in the streamwise direction down the centerline of the channel. These flow field data were only collected over rigid bed forms to ensure steady topography, as the ADV probe locally perturbed sandy bed topography. In order to determine the range of disturbance due to the presence of a single rigid bed form, the downstream flow field (Figure 1a) was measured at 0.01 m, 0.03 m and 0.06 m above the bed, and every 0.05 m in the streamwise direction. The mean velocity data showed that the reattachment point for the separated flow was located at 0.28 m or 4H downstream from the bed form crest and that a measurable momentum deficit associated with the bed form wake had fully dissipated by a distance of 1.05 m or 15H downstream from the crest (Figure 1a). These data were used for selection of bed form spacing, s, of sandy bed forms (Figure 1).

[15] Denser sets of measurements were collected over bed configurations defining cases 6b and 7b (Figure 1b). This denser grid of data was used to resolve the effects of small changes in bed topography, particularly trough shape, on flow field structure. Velocity profiles were assembled using measurements collected at several elevations, z, above the bed; at 0.005 m, and 0.01 m increments from 0.01 m to 0.07 m above the bed. The separation between adjacent profiles was 0.03 m in the streamwise (x) direction.

[16] Velocity at each point was sampled for 15 s on the basis of two lines of reasoning. First, the raw velocity data collected with the ADV can be deconvolved into three potential signals; mean, periodic and deviatoric variations [*Lyn et al.*, 1995]. For these experiments we were particularly interested in comparing the mean and deviatoric velocities between cases, so we needed to ensure that sinusoidal variations in velocity associated with the shedding of vortices at the crests of bed forms were not biasing our measurements. This was accomplished by making the sampling interval at each grid point longer than the characteristic period for vortex shedding. The duration of this period was determined by two methods. In one case the nondimensional Strouhal number, St, was used to estimate the characteristic frequency of vortex shedding. This parameter is

$$St = fD/V \tag{2}$$

where f is the characteristic frequency, D is the characteristic length and V is the characteristic velocity. Reported values of St for round and square cylinders at the appropriate Reynolds numbers (Table 2) are 0.2 [*Allen*, 1968] and 0.13 [*Lyn et al.*, 1995; *Kolár et al.*, 1997], respectively. Both cylinder geometries are considered here because they bracket the possible range of angularities associated with bed form crests. Using equation (2) a characteristic period, $1/f$, for the round and square cylinder was found by setting D equal to the original bed form height of 0.07 m and V equal to a characteristic flow velocity of 0.29 m/s (Table 2). The respective periods of 1.2 s and 1.9 s are small relative to the 15 s sampling window used at each point.

[17] Second, spectral analyses of several 120 s time series did not reveal any dominant frequency, suggesting that the actual period of vortex shedding was in fact shorter than estimated values from equation (2) and not resolvable with our experimental setup. That is, a sampling interval of 120 s

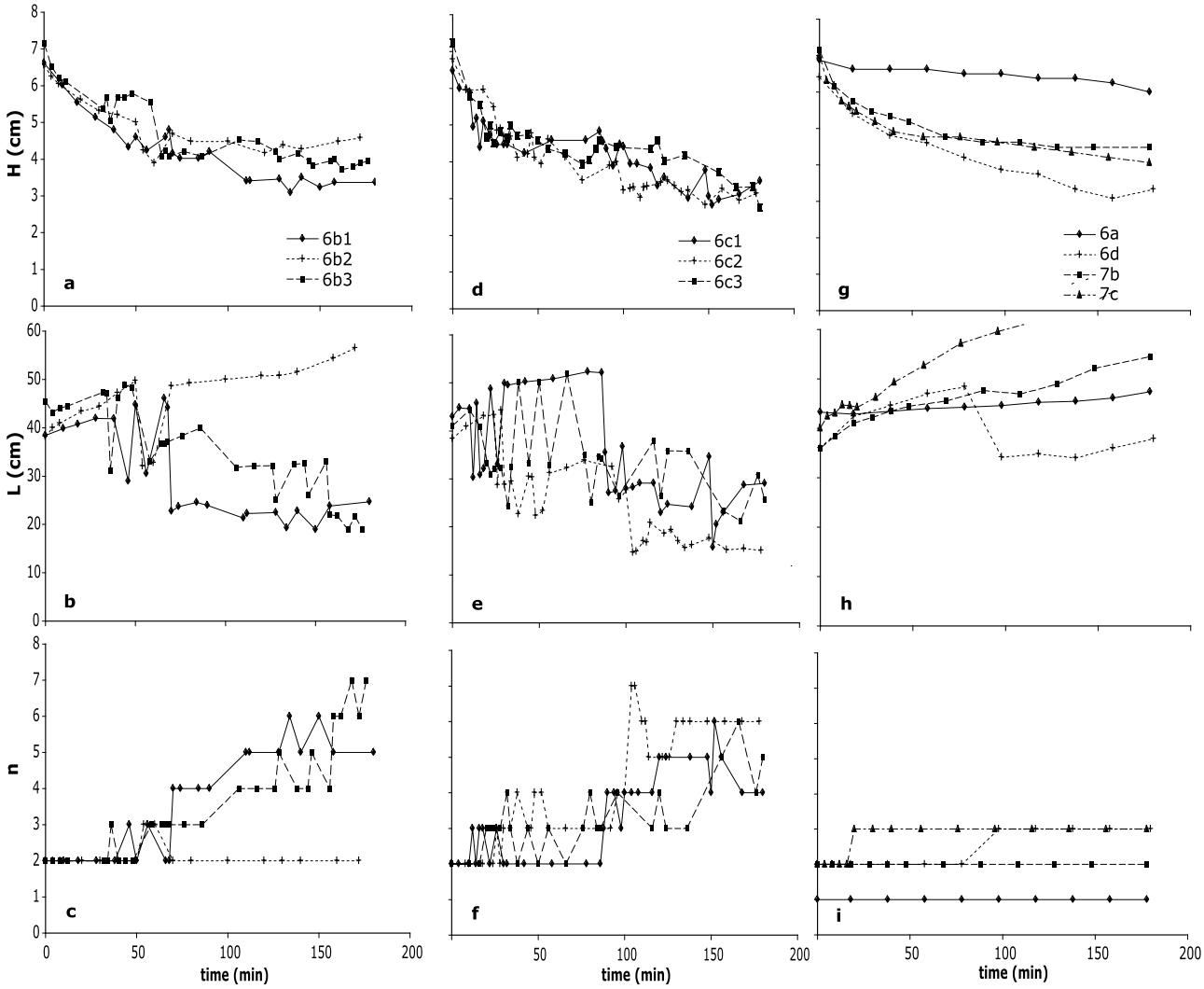

Figure 5. Time series of bed form statistics. Average bed form height (top row), average bed form length (middle row), and total number of bed forms (bottom row) for (a–c) experimental run 6b, (d–f) experimental run 6c, and (g–i) all other runs. Legends at the top of each column (Figures 5a, 5d, and 5g) indicate the run and apply to all other plots in the respective columns.

detected no longer-term oscillatory component to the flow field and produced nearly identical velocity statistics compared to a 15 s sampling interval.

[18] Mean values for the streamwise, u, and vertical, w, components of the velocity field were determined at each grid point by averaging over each 15 s sample and are denoted by $\bar{u}$ and $\bar{w}$, respectively. Deviatoric velocities associated with the streamwise and vertical components of the flow field are $u'(t) = (\bar{u} - u)$ and $w'(t) = (\bar{w} - w)$, respectively. Turbulence at any point in the flow is represented by the root mean square (RMS) of the instantaneous streamwise (RMS(u)) and vertical (RMS(w)) velocities, respectively, over the measured time interval.

3. Experimental Results

3.1. Change in Mean Bed Topography

[19] The only trend common to all runs was a reduction in mean height, the magnitude of which was similar for all runs but one (Figure 5). The outlier was case 6a, the only run with an original topography consisting of a single bed form. Change in mean height with time was not sensitive to the grain size of the original bed forms. Bed forms composed of coarse sand (cases 7b and 7c, Figure 5g) showed both the same rate of change and total height reduction as observed for all cases of two medium sand bed forms (Figures 5a, 5d, and 5g).

[20] The values for mean length either increased or decreased with time (Figures 5b, 5e, and 5h) depending on the degree to which bed form splitting occurred during a run. The average reduction in mean length for cases 6b1, 6b3, 6c1, 6c2, and 6c3 (Figures 5b and 5e) was 44%. Nearly the opposite change in mean length was observed for those cases where bed form number remained the same, in which case bed form length increased by an average of 40% from start to finish. Unlike mean height, temporal change in mean length was affected by the grain composition of the bed. All three trials with an intermediate spacing between original

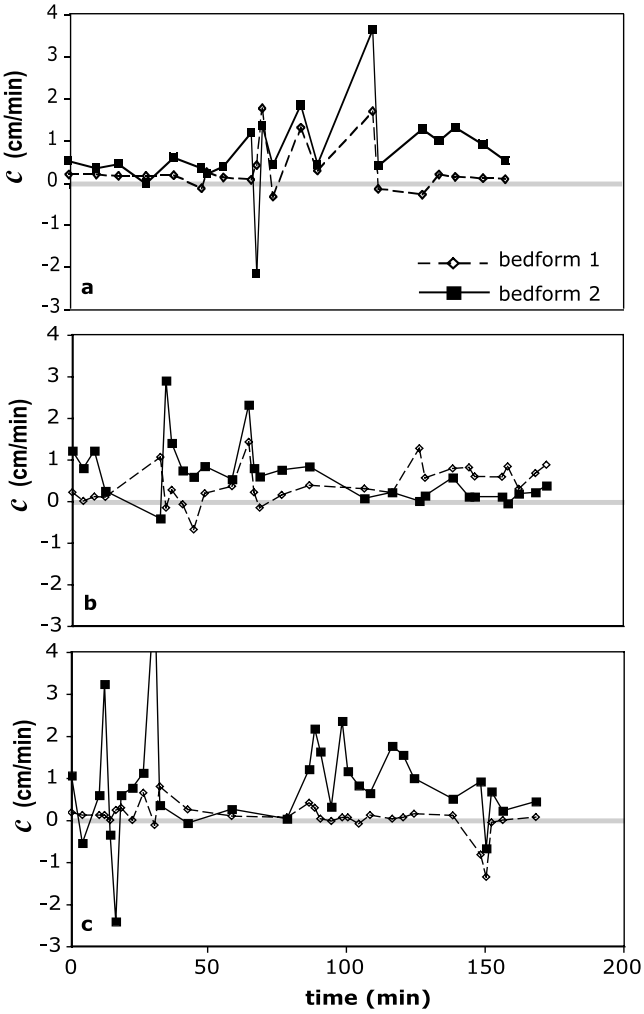

Figure 6. Episodic character of bed evolution as shown by time series of bed form celerity for runs (a) 6b1, (b) 6b2, and (c) 6c1.

bed forms composed of medium sand (case 6c) experienced a substantial increase in bed form number and the correlative reduction in mean length. This trend was not observed during the trial using coarse sand and the same original bed configuration (case 7c, Figures 5h and 5i). Almost no bed form splitting occurred in case 7c and mean length systematically increased through time. No splitting was observed for the coarse sand bed forms comprising case 7b (Figure 5i); the increase in grain size evidently suppressed bed form splitting during our runs at these low-transport conditions, as discussed below.

[21] The mean steepness (H/L) of bed topography decreased from the start to finish of each run by an amount that depended on the history of bed form splitting and length reduction. During the first ten minutes of runs 6c1, 6c2 and 6c3 the mean steepness decreased from an initial value of 0.17 to an average value of 0.14. Bed form splitting arrested this rapid drop in the overall steepness so that by the end of these three runs its average value was 0.13 (Figure 5f). Little change in steepness occurred over the rest of these runs because the smaller lengths associated with splitting offset the reductions to mean bed form height. In cases where no bed form splitting occurred, the mean steepness continued to drop throughout the runs. The special case of a single original bed form (case 6a) experienced a reduction in steepness from 0.16 to 0.13.

[22] Bed form splitting and merging are reflected in plots of bed form number (Figures 5c, 5f, and 5i). Figures 5c and 5f are particularly relevant to any consideration of the variability inherent to the bed form interface. Figures 5c and 5f each summarize the results of three runs having the same initial and boundary conditions and the plots of number versus time show significant differences.

3.2. Variability in Bed Form Evolution

3.2.1. Temporal Variability in Bed Form Activity

[23] Figures 3b and 3c illustrate increments of time associated with relatively rapid bed developments that are separated by intervals of relative stagnation (e.g., 80–100 minutes, Figure 3b: 90–110 minutes, Figure 3c). In these two series, as in all of the other experimental runs, intervals of rapid bed evolution are correlated with the splitting of preexisting bed forms. Splitting generally occurred by a process where the very front of a bed form detached from the parent bed form. The detached element typically moved forward as a new bed form while a new crest line developed near the site of the breakaway, increasing the overall number of bed forms in the system. Bed forms that emerged through the splitting process shared a height similar to that of their parent form, but a shorter length, making them steeper. Bed form celerity through time was also found to be variable. Low rates of migration were punctuated by intervals with higher rates of bed form translation (Figure 6).

3.2.2. Local and Spatial Variability in Bed Form Celerity

[24] Measurements of celerity document three main characteristics for the bed forms in our experiments: (1) Celerities of individual bed forms are independent of bed form height (Figure 7), (2) celerities are variable, and (3) higher rates of bed form migration are associated with the downstream position in the channel. Individual values for celerity (Figure 7) have been assembled to generate histograms for bed form 1 and bed form 2 (Figure 8 and Table 3). Differ-

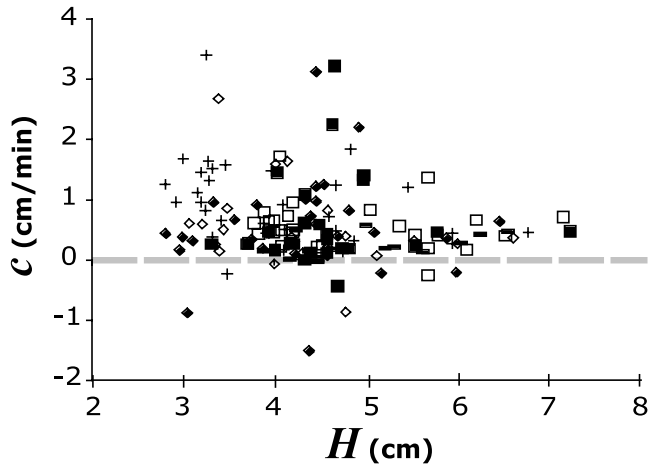

Figure 7. Bed form celerity plotted against height using all measurements from individual bed forms in all trials of cases 6b and 6c.

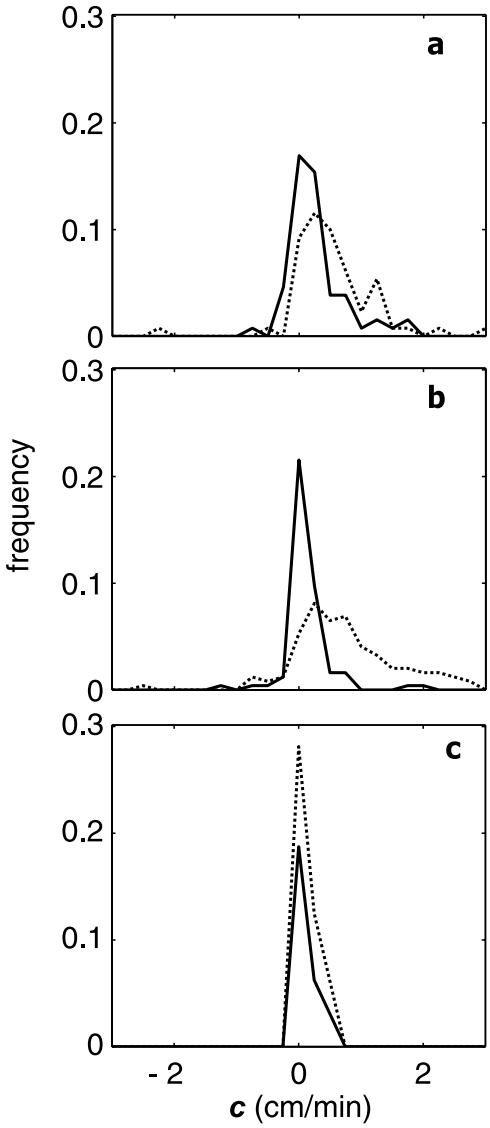

Figure 8. Histograms of bed form celerity for all forms that originated from bed form 1 (solid line) or bed form 2 (dashed line). (a) Run 6b, (b) run 6c, and (c) run 6d. The bin interval for every histogram is 0.25 cm/min. See Table 3 for statistics.

ences between the two histograms for any particular case quantify variation with streamwise position. All histograms of celerity in Figure 8 are positively skewed, and the average value for the coefficient of variation (standard deviation/mean) is greater than one. Some histograms possess negative values of celerity, which arise because any section of crest line is capable of moving backward for a short interval of time in response to minor, cross-stream variability in the transport system.

[25] Histograms (Figure 8) illustrate the influence of the original spacing between bed forms on their subsequent celerities. Measurements of celerity collected from the widely spaced bed forms in case 6d (Figure 8c) showed essentially no change between the upstream and downstream positions. Indeed, from the value of the Chi-squared parameter calculated from these two histograms we cannot reject the null hypothesis that they are indistinguishable from one another. In contrast, the histograms in Figures 8a and 8b are statistically different at the 5% confidence level. Significantly higher and more variable values of celerity were recorded in the downstream position. The closely and intermediately spaced bed forms of cases 6b and 6c lead to an overall increase in celerity from the upstream to downstream location. Maximum values of celerity in the closely and intermediately spaced configurations were always greater than those observed in the case with widely spaced bed forms.

3.2.3. Spatial Variability in Sediment Transport Rate

[26] Time-averaged values for the sediment transport (equation (1)) associated with various configurations of bed form 1 and bed form 2 define further the range in transport associated with the variable bed topography (Figure 9). Bed deformation and sediment transport was minimal in the case of a single bed form (case 6a). The presence of two bed forms in the system increased sediment transport even though there was no change in water discharge between all trials using the medium sand (Figure 9). Previously described measurements of the flow field suggested that the two bed forms in case 6d (Figure 1d) were placed far enough so that interaction between them might be negligible. This clearly was not the case. Water surface slope increased from 6×10^{-4} for case 6a, to 1×10^{-3} for the case 6d, which would cause an increase in spatially averaged bed stress, and likely caused increased sediment flux. Another cause could be a change in the structure of the flow field at a resolution finer than our coarse measurements of velocity could resolve.

[27] The enhanced transport associated with multiple bed forms was not evenly distributed down the channel. Fluxes of sediment over the crests of bed form 2 were always greater than those over bed form 1. The magnitude of this spatial difference was a function of the spacing between forms. Larger differences were measured when the two forms were placed near each other (cases 6b, 6c,

Table 3. Statistics of Time Step Averaged Bed Form Celerity for Cases 6b, 6c, and 6d[a]

Measure	Case 6b	Case 6c	Case 6d
N	130	246	24
Bed form 1 c (cm/min)	0.15, 0.28 (0.46)	0.10, 0.13 (0.37)	0.08, 0.14 (0.13)
Bed form 2 c (cm/min)	0.43, 0.57 (0.77)	0.66, 0.94 (1.19)	0.06, 0.13 (0.18)
System c (cm/min)	0.23, 0.43 (0.65)	0.26, 0.59 (1.01)	0.08, 0.14 (0.16)

[a]See Figure 8 for histograms. N = total number of celerity readings for each case; the low number of case 6d is because a smaller number of crests were generated because of less activity and also because only one trial was performed. Celerity values for each case are as follows: median, mean (standard deviation).

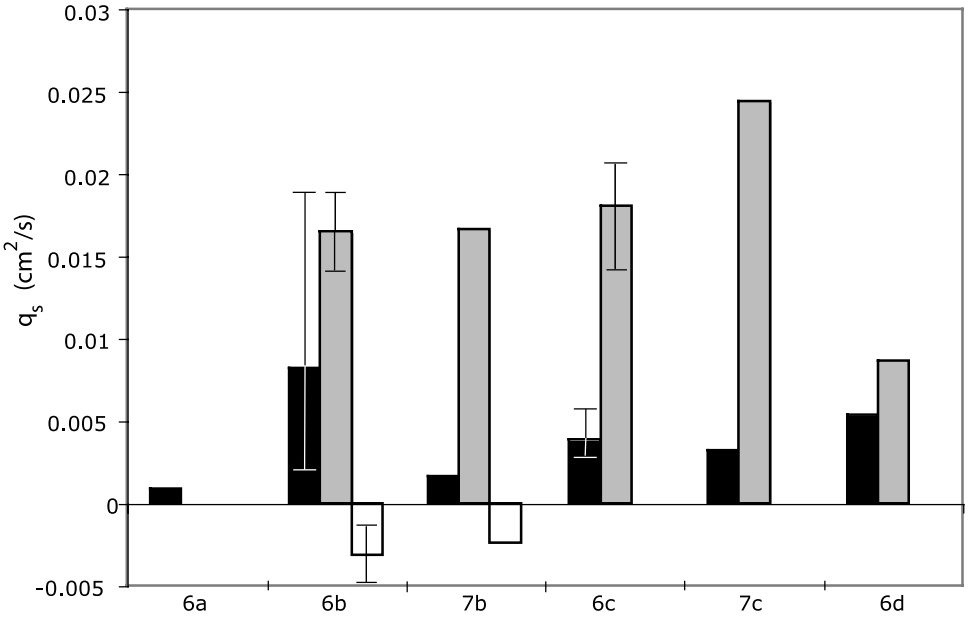

Figure 9. Local streamwise fluxes of sediment, q_s, associated with the first 1920 s of every experiment (see Figure 1 for naming convention). Solid, shaded, and open bars indicate sediment flux of bed form 1, bed form 2, and trough filling, respectively. Bars for runs 6b and 6c are each averages from 3 runs, where whiskers bracket minimum and maximum values for each case.

7b, and 7c). Little difference was measured in the case where the two bed forms had the greatest separation between them (case 6d, Figure 9). Sediment fluxes associated with the same bed configuration but a different grain size, medium versus coarse sand, are indistinguishable from each other.

[28] Measurements collected during trials with bed configurations 6b and 7b (Figure 1b) allowed us to compare

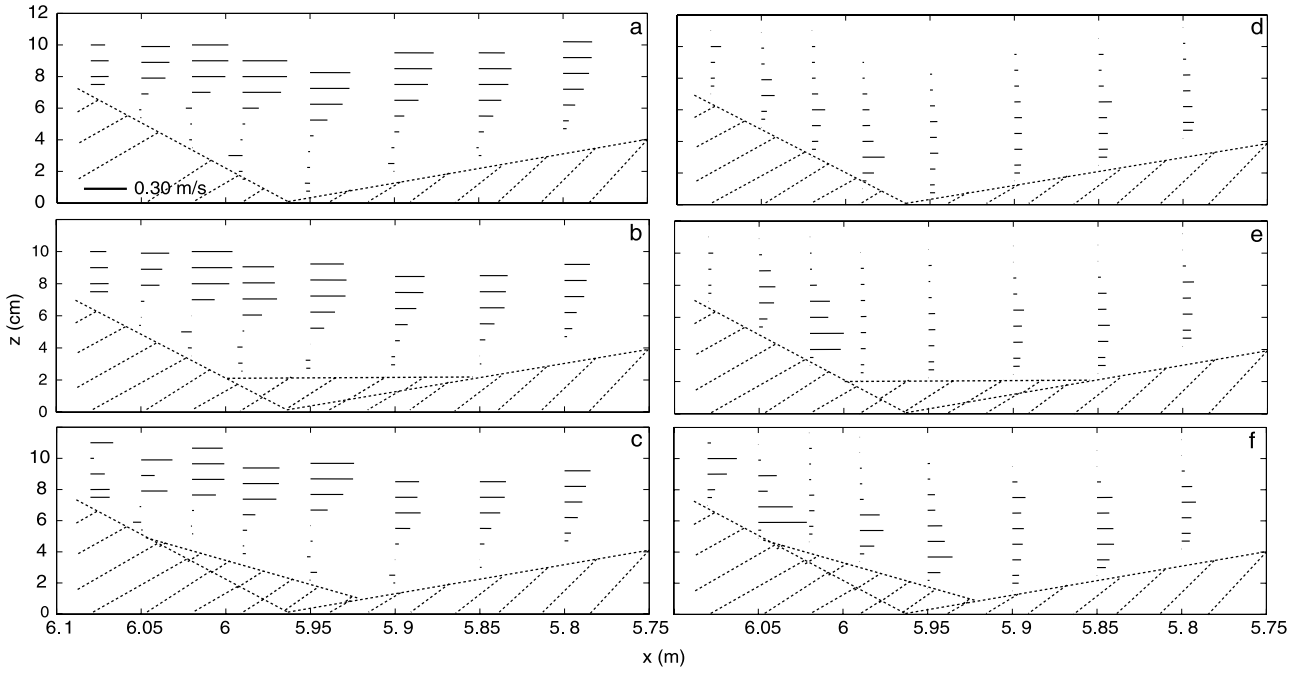

Figure 10. Flow measurements collected over two rigid bed forms placed end to end. Location is indicated in Figure 1b. Dashed lines outline the rigid bottom topography. Stick profiles defining the (a–c) mean streamwise velocity values and (d–f) streamwise RMS velocity profiles. The vertically averaged value for mean streamwise velocity in each case is 0.27 m/s. Figures 10a and 10d show mean velocity and RMS(u) associated with a simple unfilled triangular trough, Figures 10b and 10e show a horizontal plate in the trough, and Figures 10c and 10f show an inclined plate in the trough. Scale bar is shown in Figure 10a.

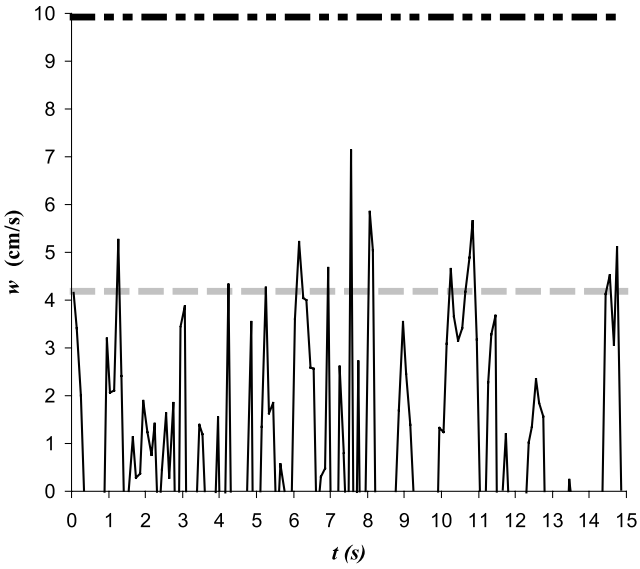

Figure 11. Upward directed instantaneous velocity, w, at $z = 5 \times 10^{-3}$ m above the bed and $x = 5.85$ m, measured for the rigid bed form case shown in Figure 10f. Also plotted are fall velocities, w_s, for medium (shaded dashed line) and coarse (solid dash-dotted line) sands.

relative magnitudes of bed form translation versus deformation. In all of these cases, the transport associated with modifying the shape of the trough separating the two bed forms was of the same order of magnitude as the transport contributing to the downstream advancement of bed form 1 (Figure 9). Visual inspection showed that sediment involved in trough filling was supplied from the stoss side of the downstream bed form, as grains ejected by turbulent bursting were swept upstream by the recirculation eddy and deposited in the trough. These comparable magnitudes highlight an intrinsic difficulty associated with measuring active bed forms. Shape changes are often large over migration distances shorter than one bed form length. Accurate characterization of bed form topography therefore requires numerous rapidly collected profiles.

3.3. Variability in the Flow Field

[29] The rapid rates of change in bed form topography illustrated in Figures 3 and 6 were preceded by relatively subtle changes in bed form shape, particularly modifications to the troughs separating adjacent bed forms. These adjustments in trough shape (Figure 4) were typically produced by sedimentation from upstream-directed transport within recirculation eddies (Figure 9). Because trough adjustments appeared to be linked to rapid deformations of the bed, we were interested in determining what modifications to the flow field were associated with different trough geometries. Three geometries were selected (Figure 10), and trough filling was characterized by first measuring the flow field over two rigid bed forms (Figures 10a and 10d). An aluminum plate was then placed in the trough and the measurements were repeated. In one case the orientation of the plate was horizontal (Figures 10b and 10e) and in another case the plate was inclined (Figures 10c and 10f). The profiles for mean velocity are remarkably similar between all three setups (Figures 10a, 10b, and 10c), whereas profiles of turbulence (RMS(u)) are different. Higher values of RMS(u) were measured for both cases with a partially filled trough (Figures 10e and 10f) compared to the original configuration (Figure 10d). Relatively small adjustments in bed form geometry produced almost no change in the mean flow field but considerable change in its turbulence structure. The largest fluctuations of u and w occurred in the bed form trough (Figure 10), and we expect these events could sweep or eject sand out of this region. Data indicate that turbulent velocity fluctuations would be much less effective at lifting coarse sand grains. Calculated settling velocity, w_s, [*Dietrich*, 1982] for d_{50} of the coarse sand (9.9 cm/s) is substantially larger than that for d_{50} of the medium sand (4.6 cm/s, Figure 11). Instantaneous vertical velocity, w, exceeds w_s of medium sand for 5% of the sample time, while never exceeding w_s of coarse sand. Although mean sediment fluxes for medium and coarse grain runs were indistinguishable (Figure 9), small but significant entrainment of grains for medium sand experiments may explain why those bed forms underwent significant splitting with large variability, whereas coarse grained bed forms simply became longer and flatter (Figure 5h).

4. Interpretation of Experimental Results

[30] Results from our experiments indicate a varied response in bed form evolution to a simple set of initial conditions. Initial bed forms were out of equilibrium with the flow field. While this situation is quite different from naturally formed topography, it allows us to amplify modes of bed form interaction that likely also operate in natural systems. The average decrease in bed form height, and the increase in length for cases where bed form splitting did not occur, is a direct result of these tall, steep bed forms responding to the imposed flow field. Two aspects of observed bed form development should be relevant to natural rivers: (1) the connection between turbulence-induced sediment transport and rapid rates of bed form evolution and (2) the influence of one bed form on adjacent bed forms.

[31] After the initiation of splitting began, the subsequent behavior of daughter bed forms appeared to depend strongly on local topography (Figure 3). We found that bed forms close in proximity can merge or split and that a bed form in the wake of an upstream form will migrate and deform more rapidly. Initial spacing of bed forms had a strong influence on subsequent evolution. Bed forms spaced very close together interacted in both upstream and downstream directions, as significant trough filling appeared to trigger splitting cascades. The process of trough filling was capable of increasing turbulent velocity fluctuations, leading to enhanced and more variable sediment transport. Although mean sediment transport rates were similar for medium and coarse grained bed forms, medium grained bed forms underwent significant splitting while coarse grained bed forms did not. We propose that the local suspension of particles in the medium sand runs produced spatial divergences in the sediment flux, driving the erosion necessary in bed form splitting. Since the threshold for suspension was never exceeded in the coarse sand runs (Figure 11), there

exists a substantial difference in morphological evolution compared to the medium sand cases.

[32] Another phenomenon explained by spatial variation in turbulence is the observed downstream increase in the sediment flux. In every case, sediment flux of bed form 2 was greater than that of bed form 1 (Figure 9), which has to do with the influence of the upstream bed form on the flow and transport field experienced by the downstream bed form. Measured RMS velocity values were larger downstream of bed form crests [see also *Nelson et al.*, 1995], and the associated developing boundary layer (Figure 1) also produced a shear stress gradient [*Nelson et al.*, 1993; *McLean et al.*, 1994], both of which enhance sediment flux. For cases 6b and 6c, this enhanced sediment flux is reflected in mean values of celerity for bed form 2, which were greater than those of bed form 1 (Figure 8 and Table 3). A surprising result is the apparent effect downstream forms have on their upstream relatives. Sediment flux of bed form 1, for every case in which two bed forms were present, is greater than that for the case of a single bed form, case 6a. Variation in celerity of the upstream bed form decreased with increasing spacing, although the differences were not statistically significant (Chi-square test, see section 3.2.2).

[33] Measurements of water depth over bed forms verified that drawdown of the water surface elevation due to acceleration over topography was small ($<10^{-3}$ m), and more importantly was equal for all bed forms for all runs. Water surface slope, however, varied by about a factor of two over the range of runs, and was not well controlled. We believe the main differences in bed form behavior among experimental runs were caused by changes in the relative position of bed forms in the turbulent flow field, but cannot rule out that small changes in water surface slope may have had an effect. Changes in water surface slope may explain observed differences in evolution of the upstream bed form under various initial conditions.

5. Conclusions

[34] We have presented results from a laboratory setup that was purposely simplified to provide unambiguous measures of how bed form dynamics are influenced by the position of an adjacent bed form. In all cases the initially tall and steep bed forms deformed rapidly in response to the imposed flow, and the manner in which bed forms adjusted was strongly influenced by the initial spacing. These measurements reveal that rates of change in bed form size and shape are sensitive to local topography. The simple initial geometry of the bed and the steady hydraulic discharge imposed on the experiments require that this variability, manifest as broad distributions in celerity and bed form geometry, was produced by the bed forms themselves.

[35] The artificial initial condition was chosen to more easily facilitate the study of bed form interaction in the laboratory. It is reasonable to question whether any results here may be generalized to the case of naturally formed bed forms. The simple fact that migration speeds of individual bed forms in a train are not equal means that interactions of the type observed here will always occur, as bed forms move in and out of the wakes induced by other bed forms. The implication is that, in sandy rivers, a bed form may be an intrinsically transient feature, as suggested by *Hersen et al.* [2004] in a model of a barchan dune field.

[36] Rapid local adjustment of bottom topography may occur where upward directed instantaneous velocity exceeds the settling velocity of grains. The interaction between bed forms depends strongly on both topography-induced flow variations and grain size. Placing this study in the context of previous work, a view emerges that the bed configuration in sandy systems is strongly influenced by smaller-scale interactions. *Coleman and Melville* [1994] observed occasional coalescence cascades where one bed form merger triggered others and suggested that this process was controlled by spacing and geometry of the bed forms involved. A similar type of behavior was observed occurring at the onset of bed form initiation from a flat bed where ripples did not develop uniformly, but rather grew fastest in the vicinity of other ripples until the entire bed surface was covered [*Coleman and Melville*, 1996]. *Gabel* [1993] found that local values of flow velocity, bed shear stress and sediment transport were highly variable, and that bed topography caused this local variability. As a result, correlations of geometry and celerity with discharge were poor.

[37] Our results bear qualitative similarities to the studies of naturally formed bed forms just described. It is difficult to quantify, however, the degree to which bed form adjustment in our experiments was driven by interactions that also occur in nature, compared to behavior driven by bed forms being out of equilibrium with the flow field. A benefit of our ''extreme condition'' setup is that it focused attention squarely on how small-scale interactions influence the bed configuration. These results motivate questions such as ''how erratic is bed form evolution in a river?'' and ''how does a river bed attain an 'equilibrium' under an imposed flow regime, and how does it adjust to a changing flow regime?'' The mechanism responsible for the apparent noise in bed form behavior is a strong nonlinear feedback between sediment transport and topography, and further exploration of the small-scale dynamics may motivate a deterministic mathematical description of river bottom self-organization. A physically realistic model describing bed form dynamics cannot be produced by averaging over the length scales of individual bed forms or timescales associated with rapid adjustment. Physical data can, however, guide development of a phenomenological model: bed forms split and merge, local adjustments act to organize the bed configuration, and all with magnitudes that may scale to mean flow properties.

[38] Our results highlight the connection between evolving topography, turbulence and sediment transport. While detailed flow measurements around static bed forms helped us to understand some of the behaviors observed in this study, we feel that topographic data are the most important information for defining the behavior of the sediment-fluid interface. To make further progress in understanding the evolution of sandy river bottom topography, field measurements must be made with a temporal and spatial resolution fine enough to resolve rapid deformation and interaction of individual bed forms. Bed forms mantling the bottoms of alluvial channels are the major source of bed roughness and help set the stage/discharge relationship for a channel at any time. Rates and styles of bed form adjustment control the evolution of the bed roughness, and hence change in stage/discharge relationships. Previous studies have, over the

decades, cataloged mean bed form geometries under a wide range of flow conditions. We suggest that future field campaigns document the lifespan, deformation rates and variability of bed forms under these same conditions. While our study does not yield any predictions for bed form evolution, it provides a motivation for examining adjustments at a finer resolution, which should contribute to more accurate predictions of their evolution. In a discussion of the effects of defects on eolian bed form dynamics, *Werner and Kocurek* [1997] posed the provocative question "Does the tail wag the dog?" In the context of subaqueous bed form geometry and sediment flux, the tails of the distributions may do a lot of the wagging.

Notation

A area of bed forms, cm^2.
c bed form celerity, cm min^{-1}.
cr bed form crest.
d representative grain diameter, μm.
D characteristic length, m.
f characteristic vortex shedding frequency, s^{-1}.
Fr Froude number = $\bar{u}\ (gh)^{-0.5}$.
g gravitational acceleration, m s^{-2}.
h water depth, m.
H bed form crest height, m.
L bed form length, m.
k porosity = 0.35.
n number of bed forms.
N number of celerity measurements.
p peak, but not a bed form.
Q_f width-averaged fluid discharge, $m^2\ s^{-1}$.
q_s 2-D sediment flux, $cm^2\ s^{-1}$.
Re Reynolds number.
s spacing of bed forms, m.
St Strouhal number = fD/V.
t time, s.
T characteristic vortex shedding period, s.
t_0 initial time, s.
t_1 arbitrary later time, s.
t_f final time for sediment flux calculations = 1920, s.
tr bed form trough.
u instantaneous streamwise velocity at a point, m s^{-1}.
$\bar{u}$ average streamwise velocity, m s^{-1}.
u' deviatoric streamwise velocity = $(\bar{u} - u)$ m s^{-1}.
u_0 velocity upstream of bed form at a point, m s^{-1}.
V characteristic velocity, m s^{-1}.
w instantaneous vertical velocity at a point, m s^{-1}.
$\bar{w}$ average vertical velocity, m s^{-1}.
w' deviatoric vertical velocity = $(\bar{w} - w)$ cm s^{-1}, m s^{-1}.
w_s particle settling velocity, cm s^{-1}.
x streamwise direction, and horizontal position, m.
y cross stream direction.
z vertical direction, and position above bed, m.
θ inclination angle between bed forms, °.
Δa area of displaced sediment, cm^2.
Δt time between chosen photographs, s.
Δx change in x over Δt, cm.

[39] **Acknowledgments.** Support for our research was provided by a Presidential Fellowship to D.J. from the Massachusetts Institute of Technology and by the STC program of the National Science Foundation via the National Center for Earth-surface Dynamics under the agreement EAR-0120914. We extend our gratitude to Ole Madson, who stimulated development of several ideas presented here. Thanks also to Chris Paola, Wes Watters, and Joel Johnson for helpful and encouraging discussions along the way. Thorough reviews by Peter Wilcock and Jonathon Nelson greatly sharpened the focus of this paper.

References

Allen, J. R. L. (1968), *Current Ripples*, Elsevier, New York.
Best, J., S. Bennett, J. Bridge, and M. Leeder (1997), Turbulence modulation and particle velocities over flat sand beds at low transport rates, *J. Hydraul. Eng.*, *123*, 1118–1129.
Carling, P. A., E. Gölz, H. G. Orr, and A. Radecki-Pawlik (2000a), The morphodynamics of fluvial sand dunes in the river Rhine, near Mainz, Germany. I. Sedimentology and morphology, *Sedimentology*, *47*, 227–252.
Carling, P. A., E. Gölz, H. G. Orr, and A. Radecki-Pawlik (2000b), The morphodynamics of fluvial sand dunes in the river Rhine, near Mainz, Germany. II. Hydrodynamics and sediment transport, *Sedimentology*, *47*, 253–278.
Coleman, S. E., and B. W. Melville (1994), Bed-form development, *J. Hydraul. Eng.*, *120*, 544–559.
Coleman, S. E., and B. W. Melville (1996), Initiation of bed forms on a flat sand bed, *J. Hydraul. Eng.*, *122*, 301–310.
Csahók, Z., C. Misbah, F. Rioual, and A. Valance (2000), Dynamics of aeolian sand ripples, *Eur. Phys. J. E*, *3*, 71–86.
Dietrich, W. E. (1982), Settling velocity of natural particles, *Water Resour. Res.*, *18*(6), 1615–1626.
Ditchfield, R., and J. Best (1992), Development of bed features, Discussion, *J. Hydraul. Eng.*, *118*, 647–650.
Endo, N., K. Taniguchi, and A. Katsuki (2004), Observation of the whole process of interaction between barchans by flume experiments, *Geophys. Res. Lett.*, *31*, L12503, doi:10.1029/2004GL020168.
Engel, P. (1981), Length of flow separation over dunes, *J. Hydraul. Div. Am. Soc. Civ. Eng.*, *107*, 1133–1143.
Gabel, S. L. (1993), Geometry and kinematics of dunes during steady and unsteady flows in the Calamus River, Nebraska, USA, *Sedimentology*, *40*, 237–269.
Harbor, D. J. (1998), Dynamics of bedforms in the lower Mississippi River, *J. Sediment. Res.*, *68*, 750–762.
Hersen, P., K. H. Anderson, H. Elbelrhiti, B. Andreotti, P. Claudin, and S. Douady (2004), Corridors of barchan dunes: Stability and size selection, *Phys. Rev. E*, *69*, 011304, doi:10.1103/PhysRevE.69.011304.
Kolár, V., D. A. Lyn, and W. Rodi (1997), Ensemble-averaged measurements in the turbulent near wake of two side-by-side square cylinders, *J. Fluid Mech.*, *346*, 201–237.
Kostaschuk, R. (2000), A field study of turbulence and sediment dynamics over subaqueous dunes with flow separation, *Sedimentology*, *47*, 519–531.
Leclair, S. F. (2002), Preservation of cross-strata due to the migration of subaqueous dunes: An experimental investigation, *Sedimentology*, *49*, 1157–1180.
Lyn, D. A., S. Einav, W. Rodi, and J. H. Park (1995), A laser-Doppler velocimetry study of ensemble-averaged statistics of the turbulent near wake of a square cylinder, *J. Fluid Mech.*, *304*, 285–320.
Maddux, T. B., J. M. Nelson, and S. R. McLean (2003a), Turbulent flow over three-dimensional dunes: 1. Free surface and flow response, *J. Geophys. Res.*, *108*(F1), 6009, doi:10.1029/2003JF000017.
Maddux, T. B., S. R. McLean, and J. M. Nelson (2003b), Turbulent flow over three-dimensional dunes: 2. Fluid and bed stresses, *J. Geophys. Res.*, *108*(F1), 6010, doi:10.1029/2003JF000018.
McLean, S. R., J. M. Nelson, and S. R. Wolfe (1994), Turbulence structure over two-dimensional bed forms: Implications for sediment transport, *J. Geophys. Res.*, *99*(C6), 12,729–12,747.
Mohrig, D. (1994), Spatial evolution of dunes in a sandy river, Ph.D. dissertation, 119 pp., Univ. of Wash., Seattle.
Nelson, J. M., S. R. McLean, and S. R. Wolfe (1993), Mean flow and turbulence fields over two-dimensional bed forms, *Water Resour. Res.*, *29*(12), 3935–3953.
Nelson, J. M., R. L. Shreve, S. R. McLean, and T. G. Drake (1995), Role of near-bed turbulence structure in bed load transport and bed form mechanics, *Water Resour. Res.*, *31*(8), 2071–2086.
Niño, Y., A. Atala, M. Barahona, and D. Aracena (2002), Discrete particle model for analyzing bedform development, *J. Hydraul. Eng.*, *128*, 381–389.
Prent, M. T. H., and E. J. Hickin (2001), Annual regime of bedforms, roughness and flow resistance, Lillooet River, British Columbia, BC, *Geomorphology*, *41*, 369–390.
Prigozhin, L. (1999), Nonlinear dynamics of Aeolian sand ripples, *Phys. Rev. E*, *60*(1), 729–733.

Schmeeckle, M. W., and J. M. Nelson (2003), Direct numerical simulation of bedload transport using a local, dynamic boundary condition, *Sedimentology*, *50*, 279–301.

Tufillaro, N. B. (1993), Discrete dynamical models showing pattern formation in subaqueous bedforms, *Int. J. Bifurcations Chaos*, *3*(3), 779–784.

van den Berg, J. H. (1987), Bedform migration and bed-load transport in some rivers and tidal environments, *Sedimentology*, *34*, 681–698.

Werner, B. T., and D. T. Gillespie (1993), Fundamentally discrete stochastic model for wind ripple dynamics, *Phys. Rev. Lett.*, *71*(19), 3230–3233.

Werner, B. T., and G. Kocurek (1997), Bed-form dynamics: Does the tail wag the dog?, *Geology*, *25*(9), 771–774.

Werner, B. T., and G. Kocurek (1999), Bedform spacing from defect dynamics, *Geology*, *25*(8), 727–730.

Wiberg, P. L., and J. M. Nelson (1992), Unidirectional flow over asymmetric and symmetric ripples, *J. Geophys. Res.*, *97*(C8), 12,745–12,761.

D. Jerolmack and D. Mohrig, Department of Earth, Atmospheric and Planetary Sciences, Massachusetts Institute of Technology, 77 Massachusetts Avenue, Cambridge, MA 02139, USA. (douglasj@mit.edu; mohrig@mit.edu)